

Contents lists available at ScienceDirect

Journal of Energy Chemistry

http://www.journals.elsevier.com/

journal homepage: www.elsevier.com/locate/jechem

Selective exchange of alkali metal ions on EAB zeolite

Yansi Tong a,b, Danhua Yuan a, Wenna Zhang a, Yingxu Wei a, Zhongmin Liu a,b,c, Yunpeng Xu a,*

- ^a National Engineering Laboratory for Methanol to Olefins, Dalian National Laboratory for Clean Energy, Dalian Institute of Chemical Physics, Chinese Academy of Sciences, Dalian 116023, Liaoning, China
- ^b University of Chinese Academy of Sciences, Beijing 100049, China
- State Key Laboratory of Catalysis, Dalian Institute of Chemical Physics, Chinese Academy of Sciences, Dalian 116023, Liaoning, China

ARTICLE INFO

Article history: Received 1 September 2020 Revised 16 September 2020 Accepted 22 September 2020 Available online 26 September 2020

Keywords: Ion exchange Alkali metal ion EAB zeolite Competitive adsorption

ABSTRACT

EAB zeolite was successfully prepared and applied to selective adsorption of Li⁺, Na⁺ and K⁺ ions. The physical and chemical properties of the adsorbent were characterized by X-ray diffraction (XRD), X-ray fluorescence (XRF), scanning electron microscope (SEM) and thermogravimetry (TG) methods. The ion exchange behaviours for Li⁺, Na⁺ and K⁺ ions in monomcomponent and multicomponent solutions were studied. In independent ion exchange, the ion exchange capacities ratios $\alpha(Na/Li)$ and $\alpha(K/Li)$ were 3.8 and 6.2, respectively. In competitive ion exchange, the selectivities $\beta(Na/Li)$ and $\beta(K/Li)$ increased with the initial concentrations and reached 409 and 992 when the initial concentrations was 100 mmol/L. The thermodynamic study results showed that Gibbs free energy change (ΔG^{Θ}) of ion exchange reaction between Li-EAB and K⁺ was -34.96 kJ/mol, indicating that ion exchange of K⁺ ions was more energetically favourable than Li⁺ ions. The calculation results showed that the energy barriers of ion exchange increased in the order K⁺ < Na⁺ < Li⁺. The study shows that EAB zeolite is potential to be used in the separation of alkali ions.

© 2020 Science Press and Dalian Institute of Chemical Physics, Chinese Academy of Sciences. Published by ELSEVIER B.V. and Science Press. All rights reserved.

1. Introduction

Seawater, as one of the most abundant resources on the earth, is a complex mixture which contains varieties of cations such as alkali metal ions and alkaline-earth metal ions [1]. After the removal of divalent metal ions, the dominant ions in seawater are Li⁺, Na⁺ and K⁺ ions [2]. Lithium is the fundamental material of lithium-ion battery, and it's demand increases steadily because of the markets expansion of cellular, computers, video cameras and cordless [3,4]. Potassium is one of the required three nutrient elements for plants, and terrestrial potassium resources are in short supply in China [5,6]. Seawater is a good resource of lithium and potassium with abundant reserves and low cost [7], so the research on separation of Li⁺, Na⁺ and K⁺ ions in a mixture solution has important value and significance.

There are many similarities in alkali metal ions' physical and chemical properties, making this separation process a challenging research topic. Adsorption method based on ion exchange has an advantage that it can be applied for the recovery of metals from the diluted seawater [2]. Many efforts have been done in past decades to separate Li⁺, Na⁺ and K⁺ ions. On highly dispersed

* Corresponding author.

E-mail address: xuyunpeng@dicp.ac.cn (Y. Xu).

zirconium phosphate, the ion exchange capacities for Li⁺, Na⁺ and K⁺ ions were 0.05, 0.38 and 0.57 mmol/g, respectively, and the separation factors $S_{\text{Na/Li}}$ and $S_{\text{K/Li}}$ maximized at 150, demonstrating the possibility of separating Li⁺ from Na⁺ and K⁺ ions [8]. On cellulose acetate fibers with supported highly dispersed aluminum phosphate, the ion exchange capacities for Li⁺, Na⁺ and K⁺ ions are 0.03, 0.44 and 0.50 mmol/g. The ion exchange selectivities were determined by difference in the hydration radii of the cations, because the smaller ionic hydration radii allow them to diffuse more easily into the solid-solution interface [9]. Polymer inclusion membrane containing a binary carrier consisting of thenoyltrifluoroacetone and trioctylphosphine oxide could high-selectively separate Li⁺, Na⁺ and K⁺ ions. The separation factors of Li⁺/Na⁺ and Li⁺/ K⁺ were 54.25 and 50.60, respectively [10]. Three ion-exchange resins (D001, LSC-100, and LSC-500) of sodium form were applied to noncompetitive and competitive adsorption of K⁺ and Li⁺ ions. In noncompetitive adsorption, the separation factors for K+/Li+ of D001, LSC-100, and LSC-500 were 3.3, 0.25 and 0.19, respectively, and in competitive adsorption, the separation factors K⁺/Li⁺ were 3.55, 0.12 and 0.094, respectively. The separation performance was attributed to the hydration energy changes, the electrostatic attractions and complexation between the alkali metal ions and the resins [11]. A cryptomelane-type hydrous manganese dioxide had extremely high selectivity to K⁺ ions. The separation factors

for K^+/Li^+ and K^+/Na^+ pairs attained 4.4 \times 10¹³ and 1.3 \times 10¹³, respectively, because the effective ionic radius of K^+ ions was approximately 1.4 Å, easily to enter the tunnel structure [12].

Zeolite is a kind of crystalline inorganic material whose framework is built up with SiO₄ and AlO₄ tetrahedra that share oxygen atoms with adjacent tetrahedra. The framework of molecular sieves are negatively charged, which are counterbalanced by cations held within the cavities and channels [13]. These cations are loosely held in the framework and can be replaced by other cations via ion exchange [14]. The ion exchange behaviors of zeolites are determined by two factors, the properties of frameworks including topology and charge density, and the properties of cations including size, shape and charge [15,16]. The ion exchange behaviors of cations are different on a specific zeolite, making it possible to apply zeolites for selective adsorption and separation of alkali metal ions.

EAB zeolite is a kind of aluminosilicate synthesized with low Si/Al ratio [17]. The EAB zeolite framework contains two types of cages, the EAB cages and GME cages, connected by 8-membered rings [18], and the aperture is 3.54 Ų [3.7 \times 5.1]. In practical operation, we found that EAB zeolite exhibited high ion exchange selectivity toward Na $^{+}$ and K $^{+}$ over Li $^{+}$ ions. Moreover, the ion exchange behaviors of EAB in monocomponent solutions were different from that in multicomponent solutions because of the competitive effect between alkali metal ions.

2. Experimental

2.1. Chemical reagent

The reagents used for synthesis including sodium aluminate (NaAlO $_2$, 51.8% Al $_2$ O $_3$), sodium hydroxide (NaOH, 96%), tetramethylammonium hydroxide (TMAOH, 25% aqueous solution), fumed silica (SiO $_2$), and reagents used for analysis including lithium chloride (LiCl, 99%), sodium chloride (NaCl, 99.8%), potassium chloride (KCl, 99.5%), were purchased from Aladdin Reagent Co., Shanghai, China. The cation standard solution (50 mg/L LiCl, 200 mg/L NaCl, 250 mg/L NH $_4$ Cl, 500 mg/L KCl) was purchased from Dionex China.

2.2. Characterization methods

Powder XRD patterns of samples were recorded using a PANalytical X'Pert PRO X-ray diffractometer with Cu K_{α} radiation (λ = 1.54059 Å). The chemical compositions of samples were determined using a Philips Magix-601 X-ray fluorescence (XRF) spectrometer. The morphologies of the samples were observed using a field emission scanning electron microscopy (SEM), Hitachi SU8020. The thermogravimetric analysis (TG) curves of samples were recorded using a TA SDT Q600 analyzer in the temperature range from room temperature to 700 °C in air stream. The concentrations of cations were determined using a Dionex ICS3000 ion chromatography system. The mobile phase was 20 mmol/L methyl sulfonic acid, the flow rate was 1.0 mL/min, the detector was a conductivity detector, the chromatographic column was a Dionex Ion- Pac^{TM} CS12A column (4 × 250 mm), the cell heater temperature was 35 °C, the column temperature was 30 °C, the suppressor type was CSRS_4 mm, the current was 77 mA.

2.3. Preparation of ion exchanger

EAB zeolite was synthetized in the same way as described by Meier [17]. At room temperature, 2.04 g fumed silica was dissolved in 20 g water, then 6.61 g templating agent TMAOH solution was added to prepare a colloidal silicon solution. Next, 0.49 g sodium aluminate and 0.40 g sodium hydroxide were dissolved in 10 g

water to prepare a clear aluminum solution. The aluminum solution was added to the silicon solution drop by drop under vigorous stirring. Then, a well-homogenized reaction mixture was obtained with a composition of 1.0Al₂O₃:13.6SiO₂:3.5Na₂O: 7.3TMAOH:1110H₂O. After being stirred for an additional 2 h, the gel was transferred into a autoclave and heated at 100 °C. After crystallization for 4 days under tumbling condition and autogenous pressure, the as-synthesized products were washed by centrifugation and dried at 120 °C. EAB zeolite has poor thermal stability and will transform into SOD zeolite above 360 °C [17]. To remove the template safely, the Na⁺ ions in the as-synthesized zeolite (Na, TMA-EAB) was almost completely replaced by K⁺ ions by 3 times ion exchange with 1 mol/L KCl solution at 80 °C for 3 h, the liquid to solid ratio was 40. Thereafter, the ion-exchanged zeolite (K, TMA-EAB) was calcined at 450 °C for 6 h. The obtained template-free zeolite (Cal-EAB) was further exchanged into NH₄ type (NH₄-EAB) or K type (K-EAB) by three times ion exchange with 1 mol/L NH₄Cl or KCl solution. In filtration process after ion exchange, the samples were washed with deionized water repeatedly until no Cl⁻ ions were detected in effluents.

2.4. Ion exchange kinetics

100 mL MCl solution was prepared in a plastic beaker, then 1 g NH₄-EAB zeolite was added to the solution under stirring. The quantity of exchangeable ions in the solution equals the theoretical ion exchange capacity of the zeolite (calculated from the the chemical composition of adsorbent). At t min, sampling from the upper solution, after filter and dilution, samples' concentrations were determined by ion chromatography. The ion exchange amount at t min was calculated by Eq. (1):

$$q_{t} = \frac{V(C_{0} - C_{t})}{m} \tag{1}$$

where $q_{\rm t}$ (mmol/g) was the ion exchange amount of the alkali metal ions, V(L) was the volume of the solutions, m(g) was the dry weight of the adsorbent, and C_0 and C_t (mmol/L) were the initial concentration and actual concentration at t min, respectively.

2.5. Ion exchange isotherm

First, 25 mL alkali metal ion solutions with different initial concentrations were prepared, and the accurate concentrations were determined by ion chromatography. Then, 0.25 g NH₄-EAB zeolite was added into the abovementioned solutions, stirring at room temperature at a rate of 350 rpm for 3 h to ensure that ion exchange equilibrium was reached (ion exchange kinetic curves were provided in Fig. S1, ion exchange equilibrium took 10 min or less, so 3 h was enough to reach equilibrium). After the zeolite particles precipitated from the suspension, the supernatant was filtered by a filter membrane. Thereafter, the equilibrium concentration was accurately determined by ion chromatography after dilution. The ion exchange amount of the alkali metal ions on the NH₄-EAB zeolite was calculated by Eq. (2):

$$q_{i} = \frac{V(C_{0,i} - C_{e,i})}{m} \tag{2}$$

where q_i (mmol/g) was the ion exchange amount of i ions, $i = \text{Li}^+$, Na^+ and K^+ , and $C_{0,i}$ and $C_{e,i}$ (mmol/L) were the initial concentration and equilibrium concentration of i ions, respectively.

2.6. Competitive ion exchange of alkali metal ions

Five mixture solutions containing equimolar Li⁺, Na⁺, and K⁺ ions were prepared. The volume was 25 mL, and the concentrations of each ion were set as 5, 10, 25, 50 and 100 mmol/L, respec-

tively (The accurate concentrations were determined by ion chromatography). Afterwards, 0.25 g NH₄-EAB zeolite was added to the above mixture solutions, stirring for 3 h to ensure that ion exchange equilibrium was reached. Then, the equilibrium concentrations of each alkali metal ion were determined by ion chromatography, and the ion exchange amounts of cations were calculated in the same way as previous Section 2.5.

2.7. Ion exchange theory study

The ion exchange reactions took place between the K-EAB zeolite and the mixture solution of KCl and MCl (M = Li, Na). The total concentration of alkali metal ions was a constant value, which equals the theoretical ion exchange capacity of the zeolite (calculated from the the chemical composition of adsorbent K-EAB, as shown in Table S1). The fractions of MCl in the initial solutions were different in each experiment. In practice, 25 mL mixture solutions were prepared with a total concentration of 32.8 mmol/L, and 0.25 g K-EAB zeolite was added to the above mixture solutions, stirring for 3 h to ensure that ion exchange equilibrium was reached. The equilibrium concentrations of alkali metal ions were the equilibrium concentrations of each alkali metal ion determined by ion chromatography, and the ion exchange amounts of Li⁺ and Na⁺ ions were determined in the same way as previous Section 2.5.

2.8. Theoretical basis

The ion exchange of K-EAB zeolite with M^+ (M = Li, Na) can be described as

$$\overline{K}^{+} + M^{+} \iff K^{+} + \overline{M}^{+}$$
 (3)

 \bar{i}^+ represents i^+ ions in the zeolite phase, i = Li, Na, K. Since the exchange reaction is reversible, the equilibrium constant K can be written as

$$K = \frac{[K^+]\overline{X}_M \gamma_K f_M}{[M^+]\overline{X}_K \gamma_M f_K} \tag{4}$$

where $[i^+]$ is the molar concentrations of i^+ ions in the solution, \overline{X}_i is the molality of i^+ ions in the zeolite phase, and γ_i and f_i represent the activity coefficients of i^+ in the solution and zeolite phase, respectively, i = M, K.

According to the law of material conservation in the solution and zeolite phase, the following relationships can be established [19].

$$X_{K} = \frac{[K^{+}]}{[M^{+}] + [K^{+}]}, X_{M} = \frac{[M^{+}]}{[M^{+}] + [K^{+}]}, [M^{+}] + [K^{+}] = TN \tag{5}$$

$$\overline{X}_K = \frac{[\overline{K}^+]}{[\overline{M}^+] + [\overline{K}^+]}, \overline{X}_M = \frac{[\overline{M}^+]}{[\overline{M}^+] + [\overline{K}^+]}, \left[\overline{M}^+\right] + \left[\overline{K}^+\right] = TN \tag{6}$$

where TN is the total molarity of all exchangeable ions in the solution, TC is the calculated total ion exchange capacity of K-EAB zeolite. When ion exchange experiments are carried out on the basis of TC = TN, Eq. (4) can be written as

$$K = \frac{(1 - X_{\rm M})\overline{X}_{\rm M}\gamma_{\rm K}}{X_{\rm M}(1 - \overline{X}_{\rm M})\gamma_{\rm M}} \frac{f_{\rm M}}{f_{\rm K}} = K_{\rm K}^{\rm M} \frac{f_{\rm M}}{f_{\rm K}} \tag{7}$$

where $K_{\rm K}^{\rm M}=\frac{(1-X_{\rm M})\overline{X}_{\rm M}\gamma_{\rm K}}{X_{\rm M}(1-\overline{X}_{\rm M})\gamma_{\rm M}}$ is defined as the corrected selectivity coefficient. $X_{\rm M}$ and $\overline{X}_{\rm M}$ can be determined by experiments, and the ratio $\gamma_{\rm K}/\gamma_{\rm M}$ can be calculated via $\gamma_{\rm KCI}/\gamma_{\rm MCI}$ using the corrected Debye-Huckel equation. When the value of $K_{\rm K}^{\rm M}$ is larger than 1, it suggests that the zeolite has a preference for M⁺ ions; when $K_{\rm K}^{\rm M}$ is smaller than 1, K⁺ ions are more preferred [12].

The experiments confirm that the ion exchange between alkali metal ions is reversible, so the Gibbs-Duhem equation can be applied to the ion exchange process [20]. The equilibrium constant K can be described as follows.

$$\ln K = \int_0^1 \ln K_K^M d\overline{X}_M + \Delta \tag{8}$$

In consideration of the experimental accuracy in practice, the term Δ is usually negligible [21]. The Kielland plot establishes the correlation between $\ln K_K^M$ and \overline{X}_M , which can be described by the following function.

$$\log K_{K}^{M} = 2C_{1}\overline{X}_{M} + \log(K_{K}^{M})_{Y_{1}, \overline{Y}_{1}, 0}$$

$$\tag{9}$$

where C_1 is the generalized Kielland coefficient. Combining Eqs. (8) and (9), constant K can be presented as

$$lnK = 2.3C_1 + ln(K_K^{M})_{X_M \overline{X}_M \to 0}$$
(10)

Thus, the thermodynamic equilibrium constant is determined by the slope C_1 and the intercept $\log(K_K^M)_{X_M\overline{X}_M\to 0}$ of the Kielland plot. The Kielland coefficient C_1 reveals the difficulties of ion exchange between the M^+ and K-EAB zeolites [19].

The Gibbs standard free energy change ΔG^{Θ} can be calculated by Eq. (11).

$$\Delta G^{\Theta} = -RT \ln K \tag{11}$$

where R is ideal gas constant, T is the ion exchange temperature.

3. Results and discussion

3.1. Characterization of the adsorbents

The XRD patterns were shown in Fig. 1. The peaks of the assynthesized sample were in good agreement with the simulated pattern of EAB zeolite derived from the single-crystal structural data, indicating that the as-synthesized sample was EAB zeolite with high purity. After direct calcination at 450 °C, the framework of as-synthesized sample collapsed and crystal phase had transformed to SOD structure, as shown in Fig. 1(5). To remove the organic templates safely, the Na^{+} ions in the as-synthesized sample

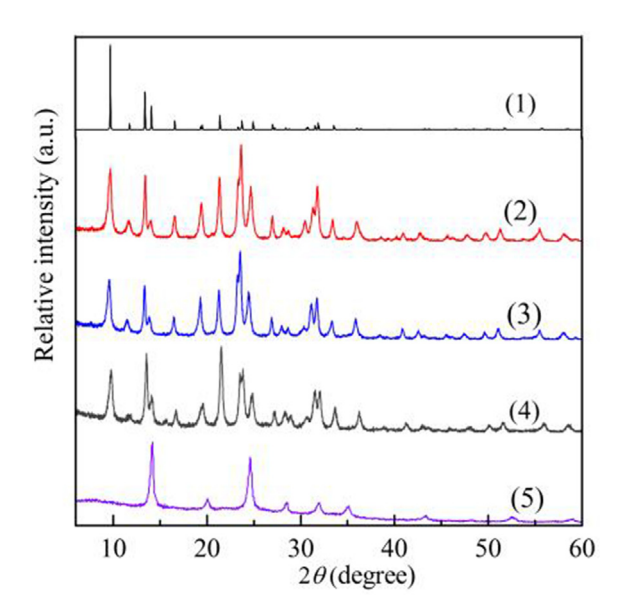


Fig. 1. XRD patterns of (1) EAB simulated from the single-crystal data, (2) assynthesized sample Na, TMA-EAB, (3) K, TMA-EAB, (4) Cal-EAB zeolite and (5) sample obtained from direct calcination of Na, TMA-EAB.

were exchanged by K^{+} ions. Taking advantage of the supporting function of K^{+} ions with larger ionic radius, EAB zeolite framework's stability was improved. The XRD patterns of Cal-EAB obtained from 450 °C calcination of K, TMA-EAB were coincident with that of the as-synthesized Na, TMA-EAB zeolite, suggesting that K, TMA-EAB zeolite could withstand high temperature up to 450 °C.

As shown in Fig. 2, EAB zeolite was highly crystallized without amorphous impurities. The micromorphology of EAB zeolite was plate-like, with a dimension of $1{\sim}3~\mu m$ in diameter and 100 nm in thickness, and some of the plates were cross-twined.

As shown in Fig. 3, the TG curves of both K, TMA-EAB and Cal-EAB had weight loss peaks from room temperature to about 200 °C, which were attributed to the evaporation of hydration water and crystallization water. The TG curve of as-synthesized K, TMA-EAB zeolite have an obvious weight loss peak ranging from 400 to 480 °C, which was attributed to the elimination of the templates. The weight loss rate was approximately 9% of dry zeolite. However, this weight loss peak was not observed on Cal-EAB's TG curve in the same temperature range, indicating that the TMA template in EAB zeolite was completely removed after calcination at 450 °C. The XRD patterns, SEM photographs and TG curves together demonstrated that EAB zeolite free of template was successfully prepared with high crystallinity and purity.

3.2. Monocomponent ion exchange isotherm

As shown in Fig. 4, the ion exchange isotherm curve of Li⁺ ions was flat. When the equilibrium concentration of Li⁺ ions was approximately 46.0 mmol/L, the ion exchange amount of Li⁺ ions reached the saturated adsorption capacity, 0.31 mmol/g, and remained unchange as the equilibrium concentration increased. The ion exchange isotherm curves of Na⁺ and K⁺ ions showed a dramatically rise in the low concentration range, and maintained an upward trend even when the initial concentration was 100 mmol/L (equilibrium concentrations were 75.2 and 88.2 mmol/L, respectively). Notably, when the initial concentration was 5 mmol/L, the ion exchange amount of Li⁺, Na⁺ and K⁺ ions were 0.04, 0.42 and 0.43 mmol/g, respectively, the selectivities α (Na/Li) and α (K/Li) were 10.5 and 10.8 at low concentration; when the initial concentration was 100 mmol/L, the ion exchange amount of Li⁺, Na⁺, K⁺ ions were 0.33, 1.25 and 2.06 mmol/g, the selectivities $\alpha(Na/Li)$ and $\alpha(K/Li)$ were 3.8 and 6.2 at high concentration. EAB zeolite has high selectivities for Na⁺ and K⁺ ions in the monocomponent ion exchange.

The channel dimension of EAB zeolite framework was 3.7×5.1 , and the calculated maximum radium of a sphere that can diffuse along the channel was 1.77 Å [22]. In aqueous solution, the permeability into the channel depended on the Stokes radii of alkali metal ions at 25 °C [23]. The Stokes radium of K⁺ ion was 1.25 Å, smaller than the calculated maximum radium; the Stokes radium

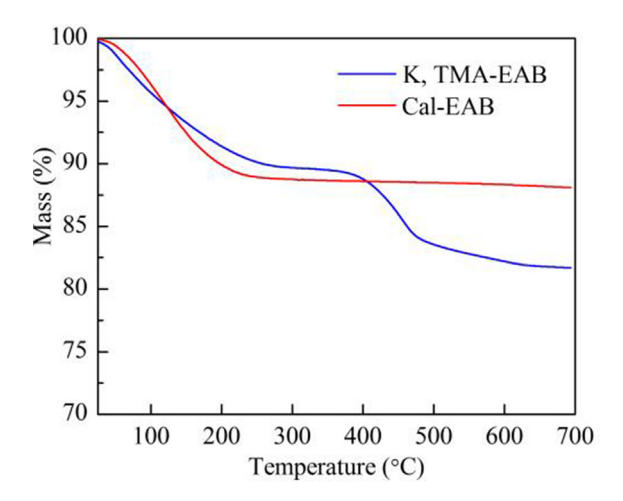


Fig. 3. TG curves of K, TMA-EAB and Cal-EAB.

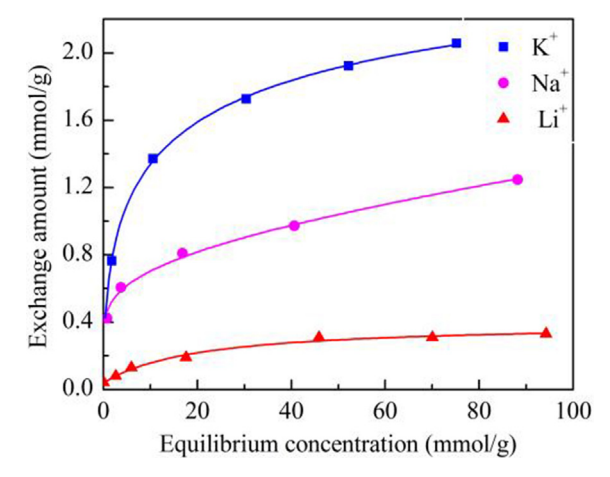


Fig. 4. Ion exchange isotherms of alkali metal ions in monocomponent ion exchange.

of Na $^+$ ion was 1.84 Å, comparable to the calculated maximum radium; and the Stokes radium of Li $^+$ ion was 2.38 Å, much bigger than the calculated maximum radium [24]. So the channel dimension of EAB zeolite was the kinetic factor for high selectivity toward Na $^+$ and K $^+$ over Li $^+$ ions.

3.3. Multicomponent competitive ion exchange

The ion exchange behavior in the multicomponent solution was different from that in the monocomponent solution. The solutions of the initial and equilibrium concentrations were shown in Fig. 5,

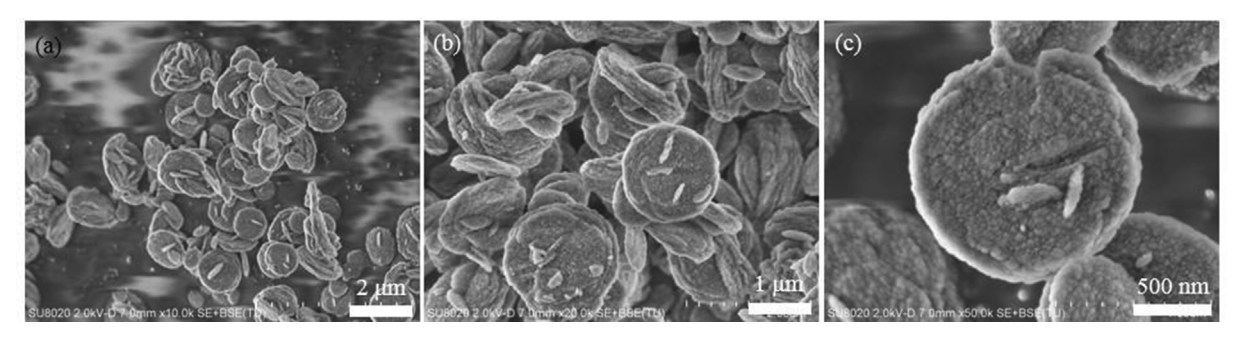


Fig. 2. SEM photographs of K-EAB zeolite at different magnifications.

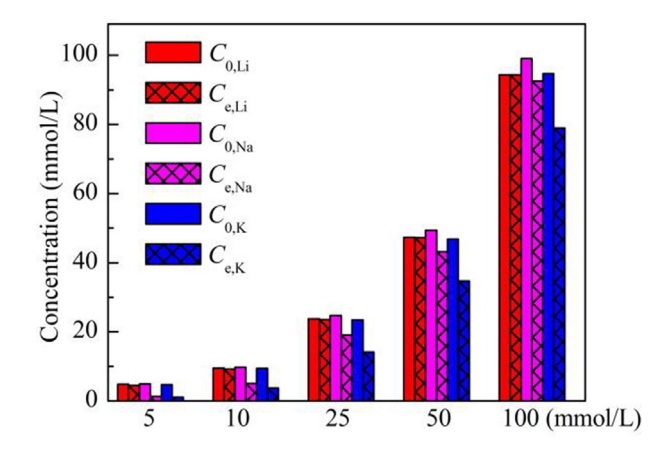


Fig. 5. Concentration changes of alkali metal ions in multicomponent ion exchange reactions.

and the ion exchange rate and selectivity were summarized in Table 1.

As shown in Fig. 5, there were significant decreases in the concentrations of Na⁺ and K⁺ ions after ion exchange in each group, but the change in concentration of Li⁺ ions was negligible. When the initial concentrations were low as 5 mmol/L, the ion exchange amounts of Li⁺, Na⁺, and K⁺ ions were 0.033, 0.360 and 0.366 mmol/g, respectively. The ion exchange selectivities β (Na/Li) and β (K/Li) were 10.8 and 11.0, respectively. The ion exchange selectivities to Na⁺, and K⁺ ions were similar to that in the monocomponent experiments at low concentrations, because there were enough sites inside the NH₄-EAB zeolite to accommodate exchange ions, and the ion exchange process of Li⁺, Na⁺, and K⁺ ions was mutually independent.

As shown in Fig. 6, when the initial concentrations of cations increased synchronously, the exchange amounts of Na⁺ and K⁺ ions both grew. The difference was that the exchange amount of Na⁺ ions almost reaches its maximum value at 50 mmol/L, but the exchange amount of K⁺ ions had an uptrend even at 100 mmol/L. In contrast, the ion exchange amount of Li⁺ ions decreased gradually along with increasing concentration of initial mixture solution. even approached zero at 100 mmol/L. The increasing ion exchange amounts of Na⁺ and K⁺ ions and decreasing amount of Li⁺ ions brought about great selectivities $\beta(Na/Li)$ and $\beta(K/Li)$, which were 409 and 992, respectively, at 100 mmol/L. In the high concentration situation, the number of cations in solution was in excess of the capacity of the zeolite, and the uptakes of cations were determined by competitive adsorption abilities of Li⁺, Na⁺, and K⁺ ions. To conclude, EAB zeolite had higher selectivities to K⁺ and Na⁺ ions than to Li⁺ ions in multicomponent competitive ion exchange, especially at high concentration.

3.4. Ion exchange theory study

In order to find out the reason for the high selectivities of Na^+ and K^+ in competitive ion exchange, the ion exchange theory was studied in detail.

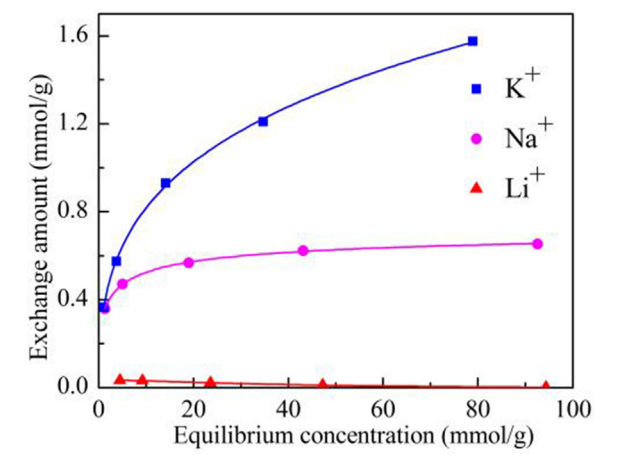


Fig. 6. Ion exchange isotherms of alkali metal ions in the multicomponent ion exchange.

Fig. 7(a) shows the isotherms of the Li $^+$ -K-EAB and Na $^+$ -K-EAB ion exchange reactions under the condition that the total normality in the solution equaled the ion exchange capacity. The isotherm curves of both Na $^+$ and Li $^+$ ions lied below the diagonal line, suggesting that EAB zeolite had a higher selectivity for K $^+$ ions than for Na $^+$ and Li $^+$ ions. Compared with the isotherm curve of Na $^+$ ions, the Li $^+$ ions' isotherm curve was much flatter, indicating that the EAB zeolite's preference for alkali metal ions was in the order Li $^+$ - \ll Na $^+$ < K $^+$, coinciding with the results in multicomponent competitive ion exchange.

Fig. 7(b) shows the Kielland plot of the Li⁺--K-EAB and Na⁺--K-EAB ion exchange reactions. Both Kielland plots had satisfactory linearity, demonstrating the rationality of the theoretical study. The $\log K_{\kappa}^{\mathrm{M}}$ on both curves was negative and decreases as the equivalent fraction in the zeolite increased, suggesting that ion exchange was becoming more difficult because an increasing number of ion exchange sites were occupied [12]. The C_1 , $\log(K_K^M)_{X_M \overline{X}_M \to 0}$ and ΔG^{Θ} of Na⁺ and Li⁺ ions exchange with K-EAB zeolite were shown in Table 2. The absolute value of the Kielland coefficient C_1 represented the energy barrier of cations entering the adsorption site as free ions. The C_1 of the Li⁺--K-EAB ion exchange was -4.97, much smaller than that in the Na⁺--K-EAB process (-0.86), indicating that ion exchange of Li+ was much more difficult than that of Na^+ ions. The calculated ΔG^Θ of the Li^+ --K-EAB ion exchange process was 34.96 kJ/mol, so this reaction was energetically unfavorable. Conversely, the ΔG^{Θ} of the reaction between K⁺ ions and Li-EAB zeolite was -34.96 kJ/mol, so K⁺ ions tended to replace Li⁺ out from the EAB framework spontaneously as follow.

$$\overline{Li}^+ + K^+ \iff Li^+ + \overline{K}^+ \tag{12}$$

where \overline{M}^+ represents specie in the adsorbent phase, M = Li, K.

At low concentrations, this replacement process rarely occurred because there were enough sites inside the EAB framework to accommodate cations. As the initial concentrations increased, on one hand, K⁺ ions would occupy more adsorption sites due to its

 Table 1

 lon exchange amounts of alkali metal ions and selectivities in multicomponent ion exchange reactions.

$C_0 \text{ (mmol/L)}$	Ion exchange amount (mmol/g)			Selectivities	
	Li ⁺	Na ⁺	K ⁺	β(Na/Li)	β(K/Li)
5	0.0332	0.360	0.366	10.8	11.0
10	0.0324	0.471	0.574	14.5	17.7
25	0.0208	0.569	0.931	27.4	44.8
50	0.0117	0.623	1.210	53.2	103
100	0.0016	0.654	1.588	409	992

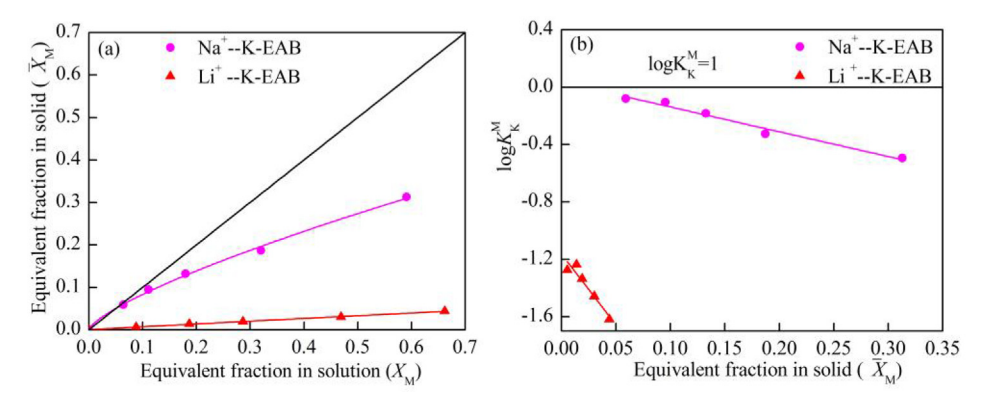


Fig. 7. (a) Isotherms of Li⁺ and Na⁺ on K-EAB zeolite when TC = TN, (b) Kielland plot of Li⁺ and Na⁺ ion exchange on K-EAB zeolite when TC = TN.

Table 2 Thermodynamic parameters of the ion exchange between K-EAB and M⁺ (M = Li, Na).

Cation	C ₁	$log(K_K^M)_{X_M,\overline{X}_M\to 0}$	ΔG^{Θ} (kJ/mol)
Na ⁺ –K-EAB	$-0.86 \\ -4.97$	0.035	4.73
Li ⁺ –K-EAB		-1.162	34.96

inherent high selectivity; on the other hand, cations replacement process occurred more frequently, leading to the increasing uptake of K^+ ions and the decreasing uptake of Li^+ ions, resulting in increasing selectivity $\beta(K/Li)$.

3.5. Ion exchange mechanism study

To gain further insight into the ion exchange mechanism, we proposed a pathway for the exchange between alkali metal ions and NH_{\bullet}^{4} .

$$mM(H_2O)_n^+ + n(NH_4^+)_{reo} \iff mM_{reo}^+ + n(NH_4^+)(H_2O)_m^+$$
 (13)

where $i(H_2O)_n^+$ represents hydrated ions in solution and i_{zeo}^+ represents i^+ ions in the zeolite phase, i = Li, Na, K, NH₄.

An ion exchange reaction can be split into two half-reactions, one of which involves NH⁴₄ ions breaking off from the framework, becoming hydrated and finally entering the solution.

$$(NH_4^+)_{zeo} \overset{\Delta H_{bind}(NH_4)}{\Longleftrightarrow} (NH_4^+)_{free}$$

$$(NH_4^+)_{free} + mH_2O \overset{\Delta H_{hydra}(NH_4)}{\Longleftrightarrow} n(NH_4^+)(H_2O)_m^+$$

$$\tag{14}$$

where ΔH_{bind} (M) is the binding energy of M⁺ entering the EAB framework, and ΔH_{hydra} (M) is the hydration energy of M⁺.

The other half-reaction involves hydrated M⁺ ions dehydrating as free ions and then entering the zeolite framework.

$$\mathsf{M}(\mathsf{H}_2\mathsf{O})_n^+ \overset{\Delta H_{hydra}(\mathsf{M})}{\Longleftrightarrow} \mathsf{M}_{free}^+ + n \mathsf{H}_2\mathsf{O}$$

$$M_{free}^{+} \stackrel{\Delta H_{bind}(M)}{\Longleftrightarrow} M_{zeo}^{+} \tag{15}$$

The reaction heat of the first half-reaction is the same for different ion exchange processes, making it ΔH_0 . The reaction heat difference comes from the latter half-reaction, which can be written

$$\Delta H_{\text{exchange}}(M) = \Delta H_0 + \Delta H_{\text{hvdra}}(M) + \Delta H_{\text{bind}}(M)$$
 (16)

Azzam calculated the $\Delta H_{\rm hydra}(M)$ by dividing the ionic heats of solvation into three contributing parts: ΔH_1 = primary solvation sheath, ΔH_2 = secondary solvation sheath, and ΔH_3 = main body

 Table 3

 Calculated enthalpy change of ion exchange reactions.

Cation	$\Delta H_{ ext{hydra}}(ext{M})$ (kJ/mol)	$\Delta H_{\mathrm{bind}}(\mathrm{M})$ (kJ/mol)	$\Delta H_{\mathrm{exchange}}(\mathrm{M})$ (kJ/mol)
Li ⁺ –NH ₄ -EAB	585.2	-894.1	$\Delta H_0 -308.9$
Na ⁺ –NH ₄ -EAB	451.6	-815.0	$\Delta H_0 -363.3$
K ⁺ –NH ₄ -EAB	354.5	-758.9	$\Delta H_0 -404.3$

of water, where ΔH_1 and ΔH_2 can be calculated by statistical-mechanical analysis, while ΔH_3 is best obtained from the Born-Bjerrum equation [25]. The theoretically calculated ionic heats of solvation were in good agreement with experimental values. The calculation method of $\Delta H_{\rm bind}({\rm M})$ of Li⁺, Na⁺, and K⁺ ions is provided in the supplementary information.

Comparing the $\Delta H_{\rm exchange}$ values in Table 3, the enthalpy change of ion exchange between M* and NH₄-EAB zeolite increased in the order $\Delta H_{\rm exchange}(K) < \Delta H_{\rm exchange}(Na) < \Delta H_{\rm exchange}(Li)$; at the same time, the energy barriers increase in the order K* < Na* < Li*, which domenstrated that the ion exchange of Na* and K* ions was energetically advantageous, in agreement with the high selectivity of the zeolite for Na* and K* ions. One the other hand, the enthalpy changes of ion exchange between Na* and K* ions and Li-EAB could be calculated from Table 3, the results were -54.4 and -95.4 kJ/mol, respectively. Under suitable conditions, such as high temperature, Na* and K* ions in solution were supposed to replace Li* ions in the EAB zeolite framework, which confirmed the high affinities to K* and Na* ions observed in the multicomponent competitive ion exchange experiments.

4. Conclusions

The ion exchange behaviors of EAB zeolite with Li[†], Na[†], and K[†] ions were investigated. Characterization results of EAB zeolite revealed that an ion exchange material was successfully prepared with high crystallinity. The EAB zeolite had high selectivities to Na[†] and K[†] ions over Li[†] ions in both monomcomponent and multicomponent ion exchange. The ion exchange theory study results showed that Na[†] and K[†] ions tended to replace Li[†] ions in the EAB framework, which was the reason for the high selectivities of Na[†] and K[†] ions. The ion exchange mechanism study results showed that the energy barriers alkali metal ions increased in an order K[†] < Na[†] < Li[†], so the ion exchange between Na[†], K[†] ions and EAB zeolite were more thermodynamically favourable. The above results show that EAB zeolite has potential application prospects in alkali ions separation.

Declaration of Competing Interest

The authors declare that they have no known competing financial interests or personal relationships that could have appeared to influence the work reported in this paper.

Appendix A. Supplementary data

Supplementary data to this article can be found online at https://doi.org/10.1016/j.jechem.2020.09.029.

References

- [1] J. Atienza, M.A. Herrero, A. Maquieira, R. Puchades, Crit. Rev. Anal. Chem. 23 (1992) 1-14.
- [2] S. Nishihama, K. Onishi, K. Yoshizuka, Solvent Extr. Ion Exch. 29 (2011) 421-431
- [3] G. Martin, L. Rentsch, M. Hock, M. Bertau, Energy Storage Mater. 6 (2017) 171-
- [4] B. Swain, J. Chem. Technol. Biotechnol. 91 (2016) 2549-2562.
- [5] N. Jin, C. Meng, J. Hou, J. Ind. Eng. Chem. 20 (2014) 1227–1230.
- [6] J. Hou, J.S. Yuan, J. Xu, L.H. Sun, Microporous Mesoporous Mat. 172 (2013) 217-

- [7] D.F. Liu, S.Y. Sun, J.G. Yu, Can. J. Chem. Eng. 97 (2019) 1589–1595.[8] C.A. Borgo, A.M. Lazarin, Y.V. Kholin, R. Landers, Y. Gushikem, J. Braz. Chem. Soc. 15 (2004) 241–247.
- [9] A.M. Lazarin, C.A. Borgo, Y. Gushikem, Y.V. Kholin, Anal. Chim. Acta 477 (2003) 305-313.
- [10] C.Q. Cai, F. Yang, Z.G. Zhao, Q.X. Liao, R.X. Bai, W.H. Guo, P. Chen, Y. Zhang, H. Zhang, J. Membr. Sci. 579 (2019) 1-10.
- T. Guo, S. Wang, X. Ye, H. Liu, X. Gao, Q. Li, M. Guo, Z. Wu, Desalin. Water Treat. 51 (2013) 3954-3959.
- [12] M. Tsuji, S. Komarneni, A. Mitsuo, Solvent Extr. Ion Exch. 11 (1993) 143-158.
- [13] A. Dyer, Stud. Surf. Sci. Catal. 157 (2005) 181-204.
- [14] R.T. Pabalan, F.P. Bertetti, Rev. Mineral. Geochem. 45 (2001) 453-518.
- [15] A. Maes, A. Cremers, ACS Symp. Ser. 323 (1986) 254-295.
- [16] R.M. Barrer, L.B. Sand, F.A. Mumpton (Eds.), Natural Zeolites: Occurrence, Properties and Uses, Pergamon Press Oxford, New York, 1978, p. 385.
- W.M. Meier, M. Groner, J. Solid State Chem. 37 (1981) 204-218
- [18] S. Cartlidge, E.B. Keller, W.M. Meier, Zeolites 4 (1984) 226-230.
- [19] T. Kodama, S. Komarneni, J. Mater. Chem. 9 (1999) 2475–2480.
- [20] G.L. Gaines, H.C. Thomas, J. Chem. Phys. 21 (1953) 714–718.
- [21] R.M. Barrer, J. Klinowski, J. Chem. Soc. Faraday Trans. 1 (70) (1974) 2080–2091.
- [22] Framework Type EAB, Database of Zeolite Framework. https://asia.izastructure.org/IZA-SC/framework.php?STC=EAB (accessed 1 October 2020)
- [23] K. Sato, T. Shiba, J. Anzai, Polymers. 5 (2013) 696-705.
- [24] E.R. Nightinga, J. Phys. Chem. 63 (1959) 1381-1387.
- [25] A.M. Azzam, Can. J. Chem. 38 (1960) 2203-2216.